



**Queensland University of Technology**  
Brisbane Australia

This is the author's version of a work that was submitted/accepted for publication in the following source:

Wu, Chengtie, [Chen, Zetao](#), Yi, Deliang, Chang, Jiang, & [Xiao, Yin](#) (2014)

Multidirectional effects of Sr, Mg and Si-containing bioceramic coatings with high bonding strength on inflammation, osteoclastogenesis and osteogenesis.

*ACS Applied Materials & Interfaces*, 6, pp. 4264-4276.

This file was downloaded from: <http://eprints.qut.edu.au/68249/>

© Copyright 2014 American Chemical Society

**Notice:** *Changes introduced as a result of publishing processes such as copy-editing and formatting may not be reflected in this document. For a definitive version of this work, please refer to the published source:*

<http://doi.org/10.1021/am4060035>

## Article

**Multidirectional effects of Sr, Mg and Si-containing bioceramic coatings with high bonding strength on inflammation, osteoclastogenesis and osteogenesis**

Chengtie Wu, Zetao Chen, Deliang Yi, Jiang Chang, and Yin Xiao

*ACS Appl. Mater. Interfaces*, **Just Accepted Manuscript** • DOI: 10.1021/am4060035 • Publication Date (Web): 05 Mar 2014Downloaded from <http://pubs.acs.org> on March 10, 2014**Just Accepted**

“Just Accepted” manuscripts have been peer-reviewed and accepted for publication. They are posted online prior to technical editing, formatting for publication and author proofing. The American Chemical Society provides “Just Accepted” as a free service to the research community to expedite the dissemination of scientific material as soon as possible after acceptance. “Just Accepted” manuscripts appear in full in PDF format accompanied by an HTML abstract. “Just Accepted” manuscripts have been fully peer reviewed, but should not be considered the official version of record. They are accessible to all readers and citable by the Digital Object Identifier (DOI®). “Just Accepted” is an optional service offered to authors. Therefore, the “Just Accepted” Web site may not include all articles that will be published in the journal. After a manuscript is technically edited and formatted, it will be removed from the “Just Accepted” Web site and published as an ASAP article. Note that technical editing may introduce minor changes to the manuscript text and/or graphics which could affect content, and all legal disclaimers and ethical guidelines that apply to the journal pertain. ACS cannot be held responsible for errors or consequences arising from the use of information contained in these “Just Accepted” manuscripts.

1  
2  
3 **dMultidirectional effects of Sr, Mg and Si-containing bioceramic coatings with high**  
4  
5 **bonding strength on inflammation, osteoclastogenesis and osteogenesis**  
6  
7

8 Chengtie Wu<sup>1,2</sup>, Zetao Chen<sup>2,3</sup>, Deliang Yi<sup>1</sup>, Jiang Chang<sup>1,2\*</sup>, Yin Xiao<sup>2,3\*</sup>  
9

10  
11 1. State Key Laboratory of High Performance Ceramics and Superfine Microstructure, Shanghai Institute of  
12 Ceramics, Chinese Academy of Sciences, 1295 Dingxi Road, Shanghai 200050, People's Republic of China  
13

14  
15 2. Australia-China Centre for Tissue Engineering and Regenerative Medicine, Queensland University of  
16 Technology, Brisbane, 60 Musk Ave, Kelvin Grove, Brisbane, Queensland 4059, Australia  
17

18  
19 3. Institute of Health and Biomedical Innovation, Queensland University of Technology, Brisbane, 60 Musk  
20 Ave, Kelvin Grove, Brisbane, Queensland 4059, Australia  
21  
22  
23

24  
25  
26 \* Corresponding authors.  
27

28 Email: jchang@mail.sic.ac.cn (J. Chang)  
29

30 Tel: +86-21-52412804; Fax: +86-21-52413903  
31  
32

33 E-mail: yin.xiao@qut.edu.au (Y. Xiao).  
34

35 Tel.: +61 7 3138 6240; fax: +61 7 3138 6030.  
36  
37

38 C.W and Z.C are co-first authors.  
39  
40  
41  
42  
43  
44  
45  
46  
47  
48  
49  
50  
51  
52  
53  
54  
55  
56  
57  
58  
59  
60

**ABSTRACT**

1  
2  
3  
4  
5  
6  
7  
8  
9  
10  
11  
12  
13  
14  
15  
16  
17  
18  
19  
20  
21  
22  
23  
24  
25  
26  
27  
28  
29  
30  
31  
32  
33  
34  
35  
36  
37  
38  
39  
40  
41  
42  
43  
44  
45  
46  
47  
48  
49  
50  
51  
52  
53  
54  
55  
56  
57  
58  
59  
60

Ideal coating materials for implants should be able to induce excellent osseointegration, which requires several important parameters, such as good bonding strength, limited inflammatory reaction, balanced osteoclastogenesis and osteogenesis, to gain well-functioning coated implants with long-term life span after implantation. Bioactive elements, like Sr, Mg and Si, have been found to play important roles in regulating the biological responses. It is of great interest to combine bioactive elements for developing bioactive coatings on Ti-6Al-4V orthopedic implants to elicit multidirectional effects on the osseointegration. In this study, Sr, Mg and Si-containing bioactive  $\text{Sr}_2\text{MgSi}_2\text{O}_7$  (SMS) ceramic coatings on Ti-6Al-4V were successfully prepared by plasma-spray coating method. The prepared SMS coatings have significantly higher bonding strength ( $\sim 37\text{MPa}$ ) than conventional pure hydroxyapatite (HA) coatings (mostly in the range of 15-25 MPa). It was also found that the prepared SMS coatings switch the macrophage phenotype into M2 extreme, inhibiting the inflammatory reaction via the inhibition of  $\text{Wnt5A}/\text{Ca}^{2+}$  and Toll-like receptor (TLR) pathways of macrophages. In addition, the osteoclastic activities were also inhibited by SMS coatings. The expression of osteoclastogenesis related genes (RANKL and MCSF) in bone marrow derived mesenchymal cells (BMSCs) with the involvement of macrophages was decreased, while OPG expression was enhanced on SMS coatings compared to HA coatings, indicating that SMS coatings also downregulated the osteoclastogenesis. However, the osteogenic differentiation of BMSCs with the involvement of macrophages was comparable between SMS and HA coatings. Therefore, the prepared SMS coatings showed multidirectional effects, such as improving bonding strength, reducing inflammatory reaction and downregulating osteoclastic activities, but maintaining a comparable osteogenesis, as compared with HA coatings. The combination of bioactive

1  
2  
3 elements of Sr, Mg and Si into bioceramic coatings can be a promising method to develop  
4  
5 bioactive implants with multifunctional properties for orthopaedic application.  
6  
7

8  
9  
10 *Key words: SMS coatings; bonding strength; osteogenesis; inflammatory reaction;*  
11  
12 *osteoclastogenesis, macrophages, bone marrow derived mesenchymal cells (BMSCs)*  
13  
14

## 15 16 17 18 **1. INTRODUCTION** 19

20 Plasma-sprayed bioactive ceramics on Ti-6Al-4V, which combines the bioactivity of  
21  
22 bioceramics and the mechanical properties of titanium alloy, have been widely used for  
23  
24 orthopaedic implant application.<sup>1-5</sup> Due to its high similarity of the bone inorganic  
25  
26 composition, hydroxyapatite (HA) has been coated on the surface of Ti-6Al-4V and achieved  
27  
28 certain clinical success. However, there are still some drawbacks arousing great attentions,  
29  
30 such as relatively low bonding strength, stability and osseointegration ability, which affect  
31  
32 its long-term clinical performance and success rate.<sup>6</sup> Bioactive glass and their composite  
33  
34 coatings have been investigated, which show good bioactivity.<sup>7-11</sup> However, it is still very  
35  
36 challenging to develop ideal bioactive ceramic-coatings on Ti alloy with excellent  
37  
38 mechanical properties (*e.g.* high bonding strength and stability) and positive biological  
39  
40 effects (*e.g.* limited inflammatory reaction, well balanced osteogenesis and osteoclastogenesis)  
41  
42 after implantation, since the osseointegration of bioactive materials with host bone tissues is  
43  
44 affected by a series of important factors, such as bonding strength, inflammatory reaction,  
45  
46 osteoclastogenesis and osteogenesis.<sup>12-17</sup>  
47  
48  
49  
50

51 The bonding strength of the coatings with substrates is an important property of coated  
52  
53 implants. Although coating materials, like HA, can well integrate with the surrounding bone  
54  
55 tissue, they also prevent the bone tissue from contacting with the titanium surface directly. It  
56  
57  
58  
59  
60

1  
2  
3 means that the bonding strength between the coating and the metal substrate surface  
4 represents most of the overall bonding strength between the implants and bone tissue before  
5 complete degradation of coating materials. Poor bonding strength may result in the  
6 delamination of coatings from Ti alloys and limits their long-term survival after  
7 implantation.<sup>18</sup> Therefore, it is of great importance to develop new coating materials which  
8 can maintain the good biological behaviours as HA while enhancing the bonding strength  
9 between coatings and metal substrates. Previous studies have shown that silicate-based  
10 bioceramic coatings generally have higher bonding strength than HA coatings prepared by  
11 plasma-spray method,<sup>3, 19, 20</sup> indicating the value of silicate bioceramics to maintain longer  
12 life span of orthopaedic implants.  
13  
14

15  
16 For the successful osseointegration, the implant is supposed to integrate with bone tissue  
17 directly without any intervening connective tissue. Inflammatory response is a key factor in  
18 determining the formation of fibrous capsule. Excessive inflammation can lead to the  
19 formation of fibrous capsule and also separate the bone cells from contacting and integrating  
20 with the implants, resulting in the failure of implants.<sup>21</sup> As foreign bodies, implants tend to  
21 cause foreign body reaction, which is known to form fibrous capsule. From this point of  
22 view, developing orthopaedic coatings with the capability of inhibiting inflammatory reaction  
23 could be a potential strategy. Macrophages are known to be one of the most important cells in  
24 the material-induced immune response to orthopaedic coatings,<sup>22</sup> thereby they can be used for  
25 investigating the interactions between bioactive coatings and immune cells.<sup>23</sup> In addition to  
26 their effects on inflammation, macrophages are also known to influence bone physiology and  
27 pathology.<sup>24, 25</sup> Macrophages are the precursors of osteoclasts, which participate in the bone  
28 remodelling and material degradation. Macrophages also contribute to osteogenesis through  
29 the expression and secretion of a wide range of regulatory molecules,<sup>26</sup> such as BMP2,  
30 transforming growth factor  $\beta$  (TGF- $\beta$ ), *etc.*<sup>27-29</sup> To our knowledge, there are few studies about  
31  
32  
33  
34  
35  
36  
37  
38  
39  
40  
41  
42  
43  
44  
45  
46  
47  
48  
49  
50  
51  
52  
53  
54  
55  
56  
57  
58  
59  
60

1  
2  
3 the osteoclastogenesis and osteogenesis induced by orthopaedic coatings with the  
4 involvement of macrophages. For these reasons, it is interesting to investigate the  
5 inflammation caused by the interaction between the coating and macrophages and the further  
6 osteoclastogenesis and osteogenesis induced by orthopaedic coatings with the involvement of  
7 macrophages.  
8  
9

10  
11  
12  
13  
14 Osteoclasts play important roles in degrading the materials and remodelling the new forming  
15 bone during osseointegration. The successful osseointegration requires adequate and effective  
16 osteoclastic activities. High osteoclastic activities may lead to the bad quality of the newly  
17 formed bone tissue (poor bone mass and density), resulting in the bad loading capacity of  
18 implants. Such a phenomenon is not uncommon clinically, especially in patients with  
19 osteoporosis. The imbalance between bone resorption and bone formation in osteoporosis  
20 patients results in high bone resorption. It is thereby of great clinical significance to develop  
21 coating materials, which are capable to inhibit osteoclastic activities, especially for patients  
22 with osteoporosis.  
23  
24  
25  
26  
27  
28  
29  
30  
31  
32  
33

34 Bone matrix deposition within the implants is another key step for the osseointegration.  
35  
36 Materials enhancing the osteogenesis would be of great significance in improving the quality  
37 of new forming bone (high bone mass and density). Osteoblasts are responsible for the  
38 deposition of bone matrix. They can also regulate the differentiation and activity of  
39 osteoclasts, thereby maintaining the skeletal architecture. In addition to their traditional  
40 effects on inflammation, immune cells are increasingly supposed to be indispensable during  
41 osteogenesis of biomaterials, with the emergence and development of osteoimmunology.<sup>29</sup>  
42  
43  
44  
45  
46  
47  
48  
49 They were found to be closely related with the bone cells, sharing a number of cytokines,  
50 receptors, signalling molecules and transcription factors.<sup>30</sup> It is reported that evaluation  
51 system for the *in vitro* osteogenesis capacity involving immune cells is more accurate than  
52 that only using osteoblastic cells.<sup>29</sup> To our knowledge, there are very few studies on the  
53  
54  
55  
56  
57  
58  
59  
60

1  
2  
3 orthopaedic coating mediating osteogenesis with the involvement of macrophages. Therefore,  
4  
5 it is interesting and more accurate to investigate the osteogenesis of bioceramic coatings by  
6  
7 using the evaluation system involving immune cells (macrophages).  
8

9  
10 For these reasons, it is interesting to coat bioactive ceramic on Ti-6Al-4V with high bonding  
11  
12 strength and the ability to inhibit the inflammatory reaction and osteoclastogenesis while  
13  
14 maintaining excellent or enhancing osteointegration. More and more evidence has shown  
15  
16 that bioactive elements play a key role in influencing the inflammatory reaction, osteogenesis  
17  
18 and osteoclastogenesis.<sup>31,32</sup> Strontium (Sr) as a trace element in human body has been found  
19  
20 to enhance osteogenesis while inhibiting osteoclastogenesis, which makes it applied widely in  
21  
22 treating osteoporosis.<sup>33-35</sup> In addition, Sr is also found to suppress the expression of the  
23  
24 inflammation-promoting cytokine interleukin 6 (IL6) and decrease the production of pro-  
25  
26 inflammatory cytokines.<sup>31, 36</sup> Magnesium (Mg) is essential for bone metabolism. The  
27  
28 depletion of Mg can affect all the stages of skeletal metabolism adversely, causing cessation  
29  
30 of bone growth, decreased osteoblastic and osteoclastic activity, osteopenia and bone  
31  
32 fragility.<sup>37,38</sup> It was also reported to decrease inflammatory cytokine production.<sup>32,39</sup> Silicon  
33  
34 (Si) is another important trace element of bone, which is reported to locate at active  
35  
36 calcification sites, involving in the mineralization process of bone growth.<sup>40</sup> Previous studies  
37  
38 have shown that the released Si-containing ionic products from bioactive glass, bioceramics  
39  
40 and coatings play an important role in stimulating the proliferation and differentiation of  
41  
42 bone-forming cells.<sup>41-43</sup>  
43  
44  
45  
46

47 To our knowledge, although Sr, Mg and Si bioactive ions elicit important effects on  
48  
49 inflammatory reaction, osteoclastogenesis or osteogenesis as well as new bone formation,  
50  
51 there are few studies to design biomaterials with these properties, especially bioceramic  
52  
53 coating materials for orthopaedic application. It is reasonable to speculate that the  
54  
55 combination of Sr, Mg and Si in the bioceramic coatings on Ti-6Al-4V may lead to the  
56  
57  
58  
59  
60



1  
2  
3 development of novel orthopaedic implants with multidirectional effects including the  
4  
5 enhancement of bonding strength, inhibition of inflammatory reaction and osteoclastogenesis,  
6  
7 and stimulation of osteogenesis. We have previously synthesized  $\text{Sr}_2\text{MgSi}_2\text{O}_7$  ceramic  
8  
9 powders.<sup>44</sup> In this study, the synthesized  $\text{Sr}_2\text{MgSi}_2\text{O}_7$  ceramic powders were coated onto the  
10  
11 Ti-6Al-4V surface employing the plasma-spray method. Systematic investigation of the  
12  
13 bonding strength of the coating on metal substrates, and the effect of the coating on  
14  
15 inflammatory reaction, osteogenesis and osteoclastogenesis as well as the possible  
16  
17 mechanisms of the effects was carried out by studying the interactions between the prepared  
18  
19 coatings and macrophages, osteoclasts and BMSCs.  
20  
21  
22  
23  
24

## 25 **2. MATERIALS AND METHODS**

### 26 *2.1 Preparation of SMS coatings on Ti-6Al-4V*

27  
28  
29 The  $\text{Sr}_2\text{MgSi}_2\text{O}_7$  (SMS) powders were synthesized by the solid-state reaction process using  
30  
31 SrO, MgO and  $\text{SiO}_2$  as raw materials according to our previous study.<sup>44</sup> To improve powder  
32  
33 flowability, a sinter-crushing method was used. Briefly, the synthesized SMS powder was  
34  
35 pressed into tablets, sintered at 1300°C. Then the sintered tablets were crushed and sieved by  
36  
37 200 and 400 meshes to obtain SMS particles with diameter of 40-80  $\mu\text{m}$  for further coating  
38  
39 preparation. The prepared SMS particles were characterized by scanning electron microscopy  
40  
41 (SEM, JSM-6700, Japan).  
42  
43  
44

45  
46 The reconstituted SMS particles were sprayed on Ti-6Al-4V (Shanghai Yantai metallic  
47  
48 material Co., Ltd, China) substrate with dimensions of 10×10×2 mm. Prior to plasma  
49  
50 spraying, the Ti-6Al-4V substrates were grit blasted, ultrasonically washed with ethanol and  
51  
52 dried at 60°C. An atmosphere plasma sprayed system (sulzer metco, Switzerland) was applied  
53  
54 to fabricate SMS coatings, and the parameters for plasma sprayed SMS coatings were shown  
55  
56 as following (argon plasma gas flow rate: 40 slpm, hydrogen plasma gas flow rate: 10 slpm,  
57  
58  
59  
60

1  
2  
3 spray distance: 120 mm, argon powder carrier gas: 3.5 slpm, current: 650 Å, voltage: 66 V).  
4  
5 HA coatings were fabricated by spraying commercial HA powders onto Ti-6Al-4V substrate  
6  
7 according to the previous study<sup>3</sup> and used as the control.  
8  
9

## 10 11 *2.2 Characterization, bonding strength and apatite mineralization of SMS coatings*

12  
13  
14 The surface microstructure of the prepared SMS coatings was observed by SEM (JSM-6700,  
15  
16 Japan). The crystal phase composition of the prepared SMS coatings was characterized by x-  
17  
18 ray diffraction (XRD, D8 advance, Bruker, Germany) using Cu K $\alpha$  radiation with scanning  
19  
20 range of 10-80° and step size 0.02°. The average linear thermal expansion coefficient of the  
21  
22 SMS-coated titanium and un-coated titanium was tested by using push-rod technique  
23  
24 according to the standard testing method GB/T 16535-2008 (Linseis L75 Platinum Series),  
25  
26 from room temperature to 800 °C.  
27  
28

29  
30 The bonding strength between SMS coatings and Ti-6Al-4V substrate was measured by a  
31  
32 mechanical tester (Instron-5592, SATEC, USA) in accordance with American Society for  
33  
34 Testing and Materials (ASTM) C-633 used in previous study.<sup>19</sup> In brief, 10 cylindrical Ti-  
35  
36 6Al-4V rods (diameter: 25.4 mm) were prepared. Half of the rods were sprayed with SMS  
37  
38 coatings, the other half were grit blasted. High-performance E-7 glue (Shanghai institute of  
39  
40 synthetic resin, Shanghai, China) was used to join the two rods (one with SMS coatings and  
41  
42 the other grit blasted), a compressive stress was applied to both rods end to assure an intimate  
43  
44 contact. The combined rods were then place into a 100 °C oven for 3 h to solidify the glue.  
45  
46 The bonding strength was measured by a mechanical tester (Instron-5592, SATEC, USA) at a  
47  
48 crosshead speed of 2 mm·min<sup>-1</sup>, and the average of five measurement was calculated for the  
49  
50 bonding strength of SMS coatings with Ti-6Al-4V substrate.  
51  
52

53  
54 To investigate the apatite-mineralization ability of the prepared SMS coatings, the coated  
55  
56 samples were immersed in acellular simulated body fluids (SBF)<sup>45</sup> and kept under shaking  
57  
58  
59  
60

1  
2  
3 conditions at 37 °C for 2, 4, 6, 8, 10, 12 and 14 days. The ionic concentrations of Sr, Si, Mg,  
4  
5 Ca and P ions released from SMS coatings were tested by inductively coupled plasma atomic  
6  
7 emission spectroscopy (ICP-AES, Varian 715ES). The formed apatite mineralization on the  
8  
9 surface SMS coatings were characterized by fourier transformed infrared spectroscopy  
10  
11 (FTIR, Nicolet Co., USA) and SEM.  
12  
13

### 14 15 16 *2.3 Cell culture*

17  
18 Three kinds of cells, including the murine-derived macrophage cell line RAW 264.7 cells,  
19  
20 osteoclasts and BMSCs were used in this study. RAW 264.7 cell cultures were maintained in  
21  
22 Dulbecco's Modified Eagle Medium (DMEM, Life Technologies, Carlsbad, California,  
23  
24 USA) supplemented with 5% fetal bovine serum (FBS, Thermo Scientific, Waltham,  
25  
26 Massachusetts, USA), and 1% (v/v) penicillin/streptomycin (Life Technologies, Carlsbad,  
27  
28 California, USA) at 37 °C in a humidified CO<sub>2</sub> incubator. The cells were passaged at  
29  
30 approximately 80% confluence by scraping and expanded through two passages before being  
31  
32 used for the study.  
33  
34

35  
36 Osteoclasts were derived from RAW 264.7 cells following the protocol as previously  
37  
38 described.<sup>46</sup> In brief, RAW 264.7 cells were seeded to the T25 flask and cultured in complete  
39  
40 medium (DMEM supplemented with 5% FBS and 1% (v/v) penicillin/streptomycin) at 37 °C  
41  
42 in a humidified CO<sub>2</sub> incubator. After three days, the medium was replaced with fresh  
43  
44 complete medium consisting of DMEM containing 5% FBS and 1% (v/v)  
45  
46 penicillin/streptomycin, and supplemented with 35 ng/ml of recombinant human RANKL  
47  
48 (Millipore, Billerica, Massachusetts, USA). Media was changed every 3 days and cells were  
49  
50 allowed to differentiate into functional osteoclasts over a period of 21 days.  
51  
52

53  
54 BMSCs were isolated and cultured based on protocols according to our previous studies.<sup>47-49</sup>

55  
56 Briefly, bone marrow was obtained from patients (50-60 years old) undergoing hip or knee  
57  
58  
59  
60

1  
2  
3 replacement surgery with informed consent given by all donors and the procedure was  
4  
5 approved by the Ethics Committee of Queensland University of Technology. Lymphoprep  
6  
7 was added to isolate the mononuclear cells from the bone marrow by density gradient  
8  
9 centrifugation (Axis-Shield PoC AS, Oslo, Norway). The obtained cells were seeded into the  
10  
11 tissue culture flasks containing DMEM supplemented with 10% FBS and 1%  
12  
13 penicillin/streptomycin and incubated at 37 °C in a humidified CO<sub>2</sub> incubator. The culture  
14  
15 medium was changed every 3 days until the primary mesenchymal cells reached 80%  
16  
17 confluence. The unattached hematopoietic cells were removed through medium change. The  
18  
19 confluent cells were routinely subcultured by trypsinisation. Only early passages (p3–5) of  
20  
21 cells were used in this study.  
22  
23  
24  
25  
26  
27

## 28 *2.4 The inflammatory response for macrophage RAW 264.7 cells cultured with SMS coatings*

### 29 *2.4.1 Inflammatory gene expression of RAW264.7 cells*

30  
31  
32  
33  
34 RAW 264.7 cells were seeded on the coating surface at a density of 10<sup>5</sup>/coating disk  
35  
36 (10×10mm). The cells were incubated for 6 days and the medium was changed on day 3. On  
37  
38 day 3 and 6, the conditioned media were collected, and centrifuged at 1500 rpm to gain the  
39  
40 supernatants. They were then mixed with complete medium at a ratio of 1:2 for the  
41  
42 conditioned-medium experiments. Total RNA was extracted using TRIzol reagent (Life  
43  
44 Technologies, Carlsbad, California, USA) on day 6 for RT-qPCR detection.  
45  
46  
47

48  
49 500 ng of total RNA was used for the synthesis of complementary DNA using DyNAmo™  
50  
51 cDNA Synthesis Kit (Finnzymes, Thermo Scientific, Waltham, Massachusetts, USA)  
52  
53 following the manufacturer's instructions. RT-qPCR primers (Table S1), which were  
54  
55 designed based on cDNA sequences from the NCBI Sequence database. SYBR Green qPCR  
56  
57 Master Mix (Life Technologies, Carlsbad, California, USA) was used for detection and the  
58  
59  
60

1  
2  
3 target mRNA expressions were assayed on the ABI Prism 7500 Thermal Cycler (Applied  
4 Biosystems, Foster City, California, USA). Each sample was performed in triplicate. The  
5 mean cycle threshold (Ct) value of each target gene was normalized against Ct value of a  
6 house keeping gene to gain the relative expression. For the calculation of fold change,  $\Delta\Delta C_t$   
7 method was applied, comparing mRNA expressions between SMS coating group and HA  
8 coating group.  
9

#### 10 11 12 13 14 15 16 *2.4.2 Flow cytometry*

17  
18 To explore the phenotype switch of macrophage, expression of M1 and M2 macrophage cell  
19 surface marker CCR7 and CD163, respectively, were determined by flow cytometry. RAW  
20 264.7 cells were seeded in the T25 flask and cultured in complete medium. After 1 day of  
21 culture, the medium was replaced by the macrophage-conditioned medium obtained from  
22 section 2.4.1. After another 2 days, the cells were detached by scraping. Nonspecific protein  
23 binding was blocked by 1% BSA/PBS. Samples were incubated with CCR7 (1:25) (GeneTex,  
24 Irvine, California, USA) and CD163 antibody (1:100) (AbD Serotec, Raleigh, North  
25 Carolina, USA) for 30 minutes at 4°C, followed by incubation with DyLight 488-anti-mouse  
26 and DyLight 405- anti-goat secondary antibody (DAKO, Multilink, California, USA) for 30  
27 minutes at 4 °C. After washing with 1% BSA/PBS, cells were analysed on a FC500 flow  
28 cytometer (Beckman Coulter, Brea, California, USA). The data were analysed using Flowing  
29 Software ([www.flowingsoftware.com](http://www.flowingsoftware.com)).  
30  
31  
32  
33  
34  
35  
36  
37  
38  
39  
40  
41  
42  
43  
44

#### 45 46 47 48 49 50 51 52 53 54 55 56 57 58 59 60 *2.4.3 Mechanism of the inflammatory gene expression change*

To understand the mechanism of two involved inflammation signalling pathways,  
Wnt5A/ $Ca^{2+}$  (Wnt5A, Fz5, calmodulin-dependent protein kinase II (CaMKII), nuclear factor  
of kappa light polypeptide gene enhancer in B-cells inhibitor, alpha ( $I\kappa B-\alpha$ )), and TLR  
pathways (MyD88, Ticam1/2,  $I\kappa B-\alpha$ ) were evaluated by RT-qPCR and Western blot. RAW  
264.7 cells were seeded on the coating surface at a density of  $10^5$ /coating disk. Total RNA

1  
2  
3 was extracted using TRIzol reagent (Life Technologies, Carlsbad, California, USA) for RT-  
4  
5 qPCR detection as described in section 2.4.1.  
6  
7

8 The whole cell lysates were collected after 7 and 24 hours of culture for the Western Blot  
9  
10 detection of CaMKII and I $\kappa$ B- $\alpha$ . 10  $\mu$ g proteins from each sample were separated on SDS-  
11  
12 PAGE gels and then transferred onto a nitrocellulose membrane (Pall Corporation, East Hills,  
13  
14 New York, USA). After being blocked in Odyssey blocking buffer for 1 hour (LI-COR  
15  
16 Biosciences, Lincoln, Nebraska, USA), the membranes were incubated with primary  
17  
18 antibodies against I $\kappa$ B- $\alpha$  (1:1000, rabbit anti-human/mouse; Cell Signaling Technology,  
19  
20 Danvers, Massachusetts, USA), CamKII (pan, 1:1000, rabbit anti-human/mouse; Cell  
21  
22 Signaling Technology, Danvers, Massachusetts, USA), and  $\alpha$ -tubulin (1:5000, rabbit anti-  
23  
24 human; Abcam, Cambridge, United Kingdom) overnight at 4 °C. The membranes were  
25  
26 washed three times in TBS-Tween buffer, and then incubated with anti-mouse/rabbit HRP  
27  
28 conjugated secondary antibodies at 1: 4000 dilutions for 1 hour at room temperature. The  
29  
30 protein bands were visualized using the Odyssey infrared imaging system (LI-COR  
31  
32 Biosciences, Lincoln, Nebraska, USA). The relative intensity of protein bands was quantified  
33  
34 using Image J software (National Institutes of Health, Bethesda, Maryland, USA).  
35  
36  
37  
38  
39  
40  
41  
42

### 43 *2.5 The osteoclastogenesis and osteoclastic activities*

44 RAW 264.7 cells and osteoclasts were seeded on the coating surface at a density of  
45  
46  $10^5$ /coating disk. On day 6, total RNA was extracted using TRIzol reagent for detection of  
47  
48 osteoclastic activities related gene expression (TRAP, Cathepsin K (CTSK), Carbonic  
49  
50 Anhydrase II (CA 2), receptor activator of NF- $\kappa$ B (RANK) and Calcitonin Receptor (CT),  
51  
52 Matrix metalloproteinase-9 (MMP9)) as described in section 2.4.1. On day 3 and 6, the  
53  
54 conditioned media were collected, and centrifuged at 1500 rpm to gain the supernatants for  
55  
56 the further ions concentration detection.  
57  
58  
59  
60

1  
2  
3 Given that osteoblastic cells are the important source of osteoclastogenesis regulating  
4 cytokines, we further used the macrophage-conditioned media to stimulate the BMSCs to  
5 detect the gene expression changes of osteoclastogenesis regulating cytokines. BMSCs were  
6 seeded in the 6 well plates and cultured in complete medium. After 1 day of culture, the  
7 medium was replaced by the macrophage-conditioned medium obtained from section 2.4.1.  
8 After 3 and 6 days, total RNA was extracted using TRIzol reagent (Life Technologies,  
9 Carlsbad, California, USA). RT-qPCR detection was carried out to determine the  
10 osteoclastogenesis regulating cytokines (MCSF, RANKL, and OPG) gene expression  
11 changes as described in section 2.4.1.  
12  
13  
14  
15  
16  
17  
18  
19  
20  
21  
22  
23  
24  
25

## 26 *2.6 The osteogenesis for BMSCs cultured with SMS coatings with involvement of immune* 27 *cells*

### 28 *2.6.1 Alkaline phosphatase activity of BMSCs*

29  
30 To detect the ALP activity of BMSCs, BMSCs were cultured in 24-well culture plates with a  
31 seeding density of 20,000 cells per well. ALP activity was assessed at 7 days culture in  
32 macrophages conditioned-coating media. The cells were lysed in 100  $\mu$ L of 0.2% Triton X-  
33 100 and then centrifuged at 14 000 rpm for 15 min at 4°C. 50  $\mu$ L supernatants were mixed  
34 with 150  $\mu$ L working solution and determined using the QuantiChrom™ Alkaline  
35 Phosphatase Assay Kit (BioAssay Systems, Hayward, California, USA). The total protein  
36 content was measured by the BCA Protein Assay Kit (Thermo Scientific, Waltham,  
37 Massachusetts, USA). The relative ALP activity was then obtained as the changed optical  
38 density (OD) values divided by the total protein content<sup>50</sup>.  
39  
40  
41  
42  
43  
44  
45  
46  
47  
48  
49  
50  
51

### 52 *2.6.2 Bone-related gene expression of BMSCs*

53  
54 BMSCs were plated at a density of 20,000 cells per well in separate 6-well plates. After 24  
55 hours of incubation, the culture medium was removed and replaced by macrophages  
56  
57  
58  
59  
60

1  
2  
3 conditioned media. Cell morphology was observed under a Nikon's inverted microscope  
4 (Eclipse Ti, Nikon, Tokyo, Japan) and figures were taken. Total RNA was extracted using  
5 TRIzol reagent after 3 and 7 days of culture for the RT-qPCR detection as described in  
6 section 2.4.1.  
7  
8  
9

### 10 11 *2.6.3 The mineralization of BMSCs*

12  
13 In order to identify mineralization nodules, Alizarin Red S staining was measured on day 14  
14 after BMSCs grown in macrophages conditioned media in a 96-well plate with osteogenic  
15 supplements. The medium was removed and the cells were washed with ddH<sub>2</sub>O and fixed in  
16 4% paraformaldehyde for 10 min at room temperature. After gently rinsing with ddH<sub>2</sub>O, the  
17 cells were stained in a solution of 2% Alizarin Red S at pH 4.1 for 20 min and were then  
18 washed with ddH<sub>2</sub>O. The samples were air-dried and figures were taken under a light  
19 microscope. The glossary of biomedical terms is listed in Table S2.  
20  
21  
22  
23  
24  
25  
26  
27  
28  
29

### 30 31 *2.7 Ionic concentrations*

32  
33 SMS and HA coated Ti-6Al-4V were immersed in the complete medium. After 3 and 6 days,  
34 the conditioned media were collected, and centrifuged at 1500 rpm to gain the supernatants,  
35 which were then mixed with 0.5% HNO<sub>3</sub> at a ratio of 1:2 for the further ions concentration  
36 detection. Macrophages and osteoclasts conditioned supernatants obtained from section 2.5  
37 were also mixed with 0.5% HNO<sub>3</sub> at a ratio of 1:2 for the further ions concentration  
38 detection. The ionic concentrations of Sr, Si, Mg, and Ca ions in complete culture medium,  
39 macrophages and osteoclasts conditioned media were quantified by inductive coupled plasma  
40 atomic emission spectrometry (ICP-AES, PerkinElmer, Waltham, Massachusetts, USA).  
41  
42  
43  
44  
45  
46  
47  
48  
49  
50  
51  
52  
53  
54  
55  
56  
57  
58  
59  
60



## 2.8 Statistical analysis

All the analyses were performed using SPSS software (IBM SPSS, Armonk, New York, USA). Data is shown as means  $\pm$  standard deviation (SD) and analysed using one-way ANOVA followed by LSD *post-hoc* test. The level of significance was set at  $P < 0.05$ .

## 3. RESULTS

### 3.1 Characterization, bonding strength and apatite mineralization of SMS coatings

Figure 1A shows the morphology of reconstituted SMS particles by sinter-crushing method. The size of the SMS particles is about 40-80  $\mu\text{m}$  with an irregular shape. The morphology of the prepared SMS coatings is shown in figure 1B and 1C. The coating has a rough surface built by random staking of fully and partially melted SMS particles (Fig. 1B). A higher magnification image presents that parts of the fully melted coating surface is relatively smooth (Fig. 1C). XRD analysis shows that the main crystal phase of prepared SMS coatings on Ti-6Al-4V is  $\text{Sr}_2\text{MgSi}_2\text{O}_7$  (JCPD 15-0016) (Fig. 1D). The average linear thermal expansion coefficient of the SMS-coated titanium and un-coated titanium in the temperature range of 20-800  $^\circ\text{C}$  was  $9.39 \times 10^{-6}$  and  $9.65 \times 10^{-6} \text{ }^\circ\text{C}^{-1}$ , respectively. The mean bonding strength of the SMS coatings with Ti-6Al-4V substrate is  $37.1 \pm 3.3$  MPa.

After soaked in SBF, there are newly formed apatite clusters on the surface of SMS coatings (Fig. 2A). Higher magnification SEM images shows that the formed clusters are composed of lath-like apatite microcrystals with the diameter of 100 nm (Fig. 2B). There are newly formed P-O characteristic peaks at the wavenumber of 1080, 603 and 562  $\text{cm}^{-1}$  in FTIR pattern after soaked SMS in SBF (Fig. 2C). Sr concentrations in SBF solution increase distinctively at the first 2 days of soaking and then decrease with the increase of soaking time. Mg and Si concentrations slightly increase at first 2 days, and then maintain a stable release. The Ca and P concentrations tend to decrease with the increase of soaking time (Fig. 2D).

### 3.2 *The inflammatory response for macrophage RAW 264.7 cells cultured with SMS coatings*

Flow cytometry results showed the mean fluorescence intensity of CD163 increased after the material stimulation (Fig. 3A a,b). On the contrary, the mean fluorescence intensity of CCR7 showed no significant changes under the same treatment (Fig. 3A c,d).

Anti-inflammatory genes IL-1ra expression was significantly upregulated by the stimulation of SMS coatings in comparison with the culture on HA coating ( $P < 0.05$ ) (Fig. 3B). On the contrary, inflammatory genes IL-1 $\beta$ , IL-6 and Oncostatin M (OSM) expression were significantly downregulated with the same treatment ( $P < 0.05$ ) (Fig. 3B).

To explore the mechanism of inflammation related gene expression changes, we examined two inflammation signalling pathways (Wnt5A/Ca<sup>2+</sup>, TLR). Both Wnt5A and Fz5 gene expression were significantly downregulated (Fig. 4A) in comparison with the HA coating group. The downstream molecules CamKII also showed significant decrease in protein expression (Fig. 4C). As to the Toll like receptor pathway, MyD88, Ticam 1 and 2 gene expression were all significantly downregulated (Fig. 4B,  $P < 0.05$ ), while the downstream molecules I $\kappa$ B- $\alpha$  were enhanced in protein expression (Fig. 4C,  $P < 0.05$ ).

### 3.3 *The osteoclastogenesis and osteoclastic activities*

Most of the osteoclastic activities related genes (TRAP, CTSK, RANK, CT, and MMP9) by macrophages were significantly downregulated by the stimulation of SMS coatings compared with that of HA coatings (Fig. 5). Similar results were observed in the stimulated osteoclasts, with the inhibitions of TRAP, CTSK, CA2, RANK, and MMP9 genes expression (Fig. 6).

The expression of RANKL, an osteoclastogenesis enhancing gene, by BMSCs under the stimulation by conditioned medium from macrophages on SMS coatings was significantly downregulated on both day 3 and day 7 (Fig. 7,  $P < 0.05$ ). MCSF, another osteoclastogenesis

1  
2  
3 enhancing gene, was also significantly downregulated on day 7 (Fig. 7,  $P < 0.05$ ).  
4  
5 Osteoclastogenesis inhibiting gene OPG showed a different pattern. It showed no significant  
6  
7 change on day 3, but was significantly upregulated on day 7 (Fig. 7,  $P < 0.05$ ).  
8  
9

### 10 11 *3.4 The osteogenesis for BMSCs cultured with SMS coatings with involvement of immune* 12 13 *cells*

14  
15 The osteogenic differentiation of BMSCs stimulated by the macrophage-conditioned medium  
16  
17 with SMS and HA coatings is shown in Figure 8. Morphology of BMSCs was similar in both  
18  
19 SMS and HA coatings groups (Fig. 8A). The ALP activity of BMSCs with SMS-stimulated  
20  
21 RAW cell medium is slightly lower than that of HA group (Fig. 8B). Bone-related genes  
22  
23 expression (ALP, OPN, OCN, COL1 and IBSP) has almost no significant difference between  
24  
25 SMS and HA coatings groups (Fig. 8C) on both day 3 and 7, (Fig. 8D). Alizarin red staining  
26  
27 shows that both SMS and HA coatings groups could lead to the formation of mineralisation  
28  
29 nodules (Fig. 8E).  
30  
31  
32  
33  
34  
35

## 36 **4. DISCUSSION**

37  
38 In this study, we successfully prepared Sr, Mg and Si-containing SMS coatings on Ti-6Al-4V  
39  
40 by plasma-spray method. For orthopaedic coating applications, the prepared coating materials  
41  
42 on titanium alloy should be relatively stable to maintain long-term life span. Although  
43  
44 bioactive glass coatings possess excellent bioactivity, their dissolution rate is generally higher  
45  
46 than that of crystallized bioceramic coatings. For this reason, we tried to combine the  
47  
48 bioactive elements of Sr, Mg and Si into the coatings to induce favourable biological effects,  
49  
50 together with higher crystallinity for higher chemical stability.  $\text{Sr}_2\text{MgSi}_2\text{O}_7$  is one of the  
51  
52 typical crystal phases in the Sr, Mg and Si containing ceramic systems. Our previous study  
53  
54 has shown that pure phase  $\text{Sr}_2\text{MgSi}_2\text{O}_7$  ceramic can be easily prepared. No phase change was  
55  
56  
57  
58  
59  
60

1  
2  
3 observed even after high temperature treatment. In addition,  $\text{Sr}_2\text{MgSi}_2\text{O}_7$  bioceramics exhibit  
4 stimulatory effects on the osteogenic differentiation of BMSCs.<sup>44</sup> Concerning these  
5 physiochemical and biological properties, we applied this kind of ceramics as orthopaedic  
6 coatings on titanium.  
7  
8

9  
10  
11 The stability of bioceramic coatings and their bonding strength with Ti alloy is of great  
12 importance to maintain their long-term life survival. When the bioceramic coated implants  
13 are implanted *in vivo*, host body cells will be in contact with the coating materials first. The  
14 coating materials will then experience some degradation either by physicochemical  
15 dissolution, cell-mediated dissolution, hydrolysis, enzymatic decomposition, or corrosion.<sup>51</sup>  
16  
17

18  
19  
20 The released ions or degraded particles from the coating are supposed to regulate the local  
21 microenvironment, which determines the response and behaviour of host cells. Therefore, it  
22 is vital to coat the titanium with bioactive materials, which can create a favourable  
23 environment for the new bone formation, like SMS did in this study. To maintain the long-  
24 term life span of the implants, bioceramic coatings should release some bioactive ions to  
25 assist the osseointegration with host bone tissue and at the same time the prepared coatings  
26 should have relatively high stability (or slow degradation). In this study, SMS showed higher  
27 osteoclastogenesis-inhibiting capacity than HA, indicating that SMS coatings may have  
28 higher biological stability than that of HA coatings. In addition to the degradation, the  
29 bonding strength of bioceramic coatings with titanium is another important factor to maintain  
30 the long-term life span of the implants, since the high bonding strength will provide a stable  
31 coating interface without delamination from titanium to support functional loading before the  
32 coating materials are completely replaced by new bone tissue.  
33  
34  
35  
36  
37  
38  
39  
40  
41  
42  
43  
44  
45  
46  
47  
48  
49  
50

51  
52 The bonding strength of HA coatings is generally in the range of 15-25 MPa.<sup>52</sup> Although the  
53 HA coated implants have achieved certain clinical success, the bonding strength of HA  
54 coating on titanic alloy is still not strong enough and may lead to the delamination  
55  
56  
57  
58  
59  
60

phenomenon in clinical applications. It is of great clinical significance to develop coated implants with high bonding strength as SMS revealed (37 MPa) in this study. Higher bonding strength of SMS coatings make them more potential for clinical applications, since they may have longer life span with functional loading.

Thermal expansion coefficient of ceramics is one of the main factors to determine the bonding strength between the coating and the metallic substrate. Previous studies have shown that the silicate-based bioceramics possess similar thermal expansion coefficient with Ti-6Al-4V, therefore favouring a higher bonding strength and reducing the residual stress due to the mismatch of the thermal expansion coefficient.<sup>3, 19, 20</sup> In this study, it is found that the SMS-coated titanium and uncoated titanium have similar linear thermal expansion coefficient. In addition, there are no obvious microcracks on the surface of SMS coatings, indicating that SMS coatings have strong bonding with titanium substrate.

In addition to their high bonding strength, SMS coatings could also switch macrophage phenotype into M2 extreme, leading to the inhibition of the inflammatory reaction compared with the HA coatings. These effects may be related to the downregulation of WNT5A/Ca<sup>2+</sup> and TLR pathways. Wnt5A/Ca<sup>2+</sup> signalling pathway is known to enhance the inflammation.<sup>53</sup> Wnt5A can bind to Fz5, activating the Wnt/Ca<sup>2+</sup> signalling pathway via CaMKII and protein kinase C, which culminates the expression of downstream inflammatory cytokine genes via the transcription factor NFκB.<sup>53</sup> After soaked SMS coated implants, the culture medium showed a significant decrease of Ca<sup>2+</sup> concentration. It is a logical extension to speculate that the decrease of Ca<sup>2+</sup> concentrations may lead to the inhibition the Wnt/Ca<sup>2+</sup> signalling pathway, resulting in the anti-inflammatory effects.

Macrophages recognize the foreign bodies via TLR pathway, inducing innate immune response trying to degrade or reject the implants.<sup>54</sup> MyD88 is one of the key components in this pathway. Most of the activated TLRs interact with MyD88, which then activate

1  
2  
3 downstream cascade.<sup>55</sup> However, TLR3 can only conduct through a MyD88-independent  
4 signalling pathways, toll-like receptor adaptor molecule (Ticam), also known as TIR domain  
5 containing adapter inducing IFN  $\beta$  (TRIF), while TLR4 can signal through both pathways.<sup>56</sup>  
6  
7 Although producing signal through different adapter proteins, both MyD88-dependent and  
8 Ticam-dependent pathways eventually activate the NF- $\kappa$ B, resulting in the expression of  
9 inflammatory cytokines.<sup>57</sup> In the present study, MyD88, Ticam1 and Ticam2 gene  
10 expressions were all downregulated, while the NF $\kappa$ B inhibitor I $\kappa$ B was upregulated. It means  
11 that the SMS coatings might also lead to the inhibition of inflammatory response via TLR  
12 pathway. After the immersion of SMS coated implants, the culture medium showed a  
13 significant increase of Mg<sup>2+</sup> concentration. Mg was known to suppress inflammatory  
14 cytokine production through inhibition of TLR pathway.<sup>32</sup> Therefore, the inhibition of this  
15 pathway might be related to the release of Mg<sup>2+</sup> from SMS coatings. Sr<sup>2+</sup> is also found to  
16 decrease inflammatory cytokine production, which was also increased in the culture medium  
17 after soaked SMS coated implants.<sup>31,36</sup> However, the underlying mechanism is still unknown.  
18  
19 Nevertheless, the inhibition of inflammatory response indicates that the SMS coatings are  
20 more compatible than HA coatings, which may prevent the formation of fibrous capsule.  
21  
22

23  
24  
25  
26  
27  
28  
29  
30  
31  
32  
33  
34  
35  
36  
37  
38  
39 The osteoclastogenesis and osteoclastic activities were both inhibited by SMS coatings. The  
40 interactions between SMS coatings with pre-osteoclasts (macrophages), and osteoclasts were  
41 firstly investigated. Our results showed that SMS coatings significantly downregulated the  
42 osteoclast activity-related genes of both pre-osteoclasts (macrophages) and osteoclasts, such  
43 as TRAP, CTSK, RANK, and MMP9. Osteoblastic cells are also known to regulate the  
44 osteoclastogenesis via the releasing of RANKL, MCSF and OPG. MCSF binds to its receptor,  
45 c-fms, on osteoclast precursors and activates signalling through Akt and MAP kinases  
46 pathway.<sup>58</sup> RANKL binds to RANK, receptor on the surface of osteoclast precursors,  
47 activating signalling through NF- $\kappa$ B, activator protein 1 (AP-1) and nuclear factor of  
48  
49  
50  
51  
52  
53  
54  
55  
56  
57  
58  
59  
60

1  
2  
3 activated T cells 2 to induce expression of genes for the survive and differentiation of  
4 osteoclasts.<sup>59</sup> OPG, a decoy receptor derived from osteoblasts, can bind to RANKL and  
5 interrupt its interaction with RANK receptor, thereby inhibit the osteoclastogenesis.<sup>60, 61</sup>  
6  
7 Therefore, we further investigated the expression of RANKL, MCSF and OPG genes in  
8 BMSCs cultured in the conditioned media. It was found that SMS coatings could decrease the  
9 expression of RANKL and MCSF genes, and increase OPG expression of BMSCs. All these  
10 results suggest that SMS coatings downregulate the osteoclastogenesis and osteoclastic  
11 activities, as compared to HA coatings.  
12  
13  
14  
15  
16  
17  
18  
19

20  
21 It is found that  $\text{Sr}^{2+}$  and Sr-containing biomaterials have inhibitory effect on the osteoclastic  
22 differentiation and resorptive activity.<sup>62, 63</sup> The underlying mechanism might be related to the  
23 suppression of IL6 family of cytokines.<sup>36</sup> IL-6 and OSM are IL6-type cytokines that stimulate  
24 osteoclast formation and function, which were both downregulated in this study. IL6 is  
25 believed to play a positive regulatory role in osteoclast differentiation by inducing the  
26 expression of RANKL on the surface of osteoblasts, activating the RANK signalling pathway  
27 on osteoclast progenitors.<sup>64</sup> The inhibition of IL6 receptor can directly block the osteoclast  
28 formation.<sup>65</sup> OSM uses the same receptor subunit, gp130, for signaling, and often have  
29 similar and overlapping functions with IL6.<sup>66</sup> OSM can help to enhance the  
30 osteoclastogenesis in a dose dependent manner, which might be related to its synergistic  
31 effects with IL6.<sup>67</sup>  
32  
33  
34  
35  
36  
37  
38  
39  
40  
41  
42  
43  
44  
45

46 In this study, the concentrations of the released  $\text{Sr}^{2+}$  in the macrophage-conditioned medium  
47 reach 134 ppm for SMS coatings, which are significantly higher than those for HA coatings  
48 (only 0.25 ppm) (as shown in Table 1). Therefore, it is reasonable to speculate that the  
49 possible mechanism for the downregulated osteoclastogenesis of SMS coatings is mostly  
50 relative to the released  $\text{Sr}^{2+}$  ions from coatings. The inhibition of osteoclastogenesis may help  
51 to obtain properly balanced osteoclastogenesis and osteogenesis, extending the applications  
52  
53  
54  
55  
56  
57  
58  
59  
60

1  
2  
3 of SMS coated Ti-6Al-4V to the patients with harsh bone qualities (low bone mass and  
4  
5 density), especially those with osteoporosis.  
6  
7

8  
9 Previous studies have found that ionic products (Si, Mg, Sr) from SMS powders could  
10 enhance the osteogenesis of BMSCs.<sup>44</sup> It is known that the ion release from crystalline  
11 materials is mainly due to the dissolution of the materials in the aqueous environment. The  
12 dissolution rate of the crystalline materials mainly depends on the chemical composition and  
13 crystal structure. In this study, we found that although the dissolution of SMS coatings was  
14 slow, it did release Sr, Mg and Si ions, which induces the favourable biological effects. Given  
15 to the importance of immune cells during the material stimulated osteogenesis, we further  
16 investigated the osteogenesis-inducing capacity of SMS coatings with the involvement of  
17 immune cells (macrophages). It was found that the osteogenic differentiation of BMSCs on  
18 SMS coatings was comparable to that on the HA coatings even with the involvement of  
19 macrophages, indicating that SMS coatings have comparable *in vitro* osteogenesis-inducing  
20 capacity to HA coatings. Previous studies for evaluation of the *in vitro* osteogenesis mainly  
21 focused on the interaction of osteoblastic cells with bioactive coatings.<sup>68, 69</sup> Current study  
22 extends the method by involving the macrophages to investigate the osteogenesis of BMSCs  
23 cultured with SMS coatings, which makes the evaluation for the *in vitro* osteogenesis-  
24 inducing capacity of SMS coatings more sufficient and accurate.  
25  
26  
27  
28  
29  
30  
31  
32  
33  
34  
35  
36  
37  
38  
39  
40  
41  
42  
43

44 After implanted, the coating materials will be completely degraded eventually and replaced  
45 by new bone tissue. The degradation time differs from the composition and structure of the  
46 materials. It means that coating materials will exist temporarily during the integration of  
47 titanium substrate with host bone tissue. Titanium materials are not very effective to guide  
48 the regeneration of surrounding tissue. Coating with bioactive materials can well solve this  
49 issue, endowing titanium with bioactivities. The major function of coating materials is to  
50 regulate an osteogenesis-enhancing environment for better integration of the titanium  
51  
52  
53  
54  
55  
56  
57  
58  
59  
60



1  
2  
3 substrate with host bone tissue. One shortcoming of this strategy is creating one more  
4  
5 interface temporarily between titanium substrate and coating materials. The bonding strength  
6  
7 should be strong enough for keeping the implants steady before the replacement of coating  
8  
9 materials with new bone tissue, which makes the bonding strength between coating materials  
10  
11 and metallic substrate a very important property of coating materials. HA has good  
12  
13 bioactivities; however, the interface between HA and titanium substrate is not strong enough  
14  
15 in bonding strength limiting its application, while the new SMS coatings seems to overcome  
16  
17 this problem with significantly higher bonding strength.  
18  
19  
20  
21  
22  
23  
24

## 25 **5. CONCLUSIONS**

26  
27 In this study, bioactive elements Sr, Mg and Si-containing SMS coatings on Ti-6Al-4V have  
28  
29 been successfully prepared by plasma-spray method. The prepared SMS coatings possess  
30  
31 significantly higher bonding strength than that of HA coatings. SMS coatings inhibit the  
32  
33 inflammatory reaction of immune cells RAW 264.7 possibly via the inhibition of  
34  
35 WNT5A/Ca<sup>2+</sup> and TLR pathways. In addition, SMS coatings could also inhibit the  
36  
37 osteoclastic activities and osteoclastogenesis while maintaining good osteogenesis-inducing  
38  
39 capacity. These multidirectional effects suggest that the SMS-coated Ti-6Al-4V may be a  
40  
41 promising implant material for the orthopaedic applications.  
42  
43  
44  
45  
46

## 47 **Acknowledgements**

48  
49 Funding for this study was provided by the Recruitment Program of Global Young Talent,  
50  
51 China (C.W.), Shanghai Pujiang Talent Program (12PJ1409500), Natural Science Foundation  
52  
53 of China (Grant 31370963, 81201202 and 81190132), Innovative Project of SIC, CAS,  
54  
55 NHMRC (APP1032738) and ARC (DP120103697).  
56  
57  
58  
59  
60

1  
2  
3  
4  
5 Associated Content  
6

7 Supporting Information Available: Glossary of biomedical terms and qPCR primers used in  
8 this paper. This material is available free of charge via the Internet at <http://pubs.acs.org>.  
9  
10

11  
12  
13  
14 **References**  
15

- 16 1. Roy, M.; Fielding, G. A.; Beyenal, H.; Bandyopadhyay, A.; Bose, S. Mechanical, in  
17 vitro antimicrobial, and biological properties of plasma-sprayed silver-doped hydroxyapatite  
18 coating. *ACS Appl. Mater. Interfaces* 2012, 4, 1341-1349.  
19  
20  
21  
22 2. Chung, C. J.; Long, H. Y. Systematic strontium substitution in hydroxyapatite  
23 coatings on titanium via micro-arc treatment and their osteoblast/osteoclast responses. *Acta*  
24 *Biomater.* 2011, 7, 4081-4087.  
25  
26  
27  
28 3. Wu, C.; Ramaswamy, Y.; Liu, X.; Wang, G.; Zreiqat, H. Plasma-sprayed CaTiSiO<sub>5</sub>  
29 ceramic coating on Ti-6Al-4V with excellent bonding strength, stability and cellular  
30 bioactivity. *J. R. Soc. Interface* 2009, 6, 159-168.  
31  
32  
33  
34 4. Balani, K.; Anderson, R.; Laha, T.; Andara, M.; Tercero, J.; Crumpler, E.; Agarwal,  
35 A. Plasma-sprayed carbon nanotube reinforced hydroxyapatite coatings and their interaction  
36 with human osteoblasts in vitro. *Biomaterials* 2007, 28, 618-624.  
37  
38  
39  
40 5. Wu, S.; Liu, X.; Yeung, A.; Yeung, K. W.; Kao, R. Y.; Wu, G.; Hu, T.; Xu, Z.; Chu,  
41 P. K. Plasma-modified biomaterials for self-antimicrobial applications. *ACS Appl. Mater.*  
42 *Interfaces* 2011, 3, 2851-2860.  
43  
44  
45  
46 6. Khor, K. A.; Gu, Y. W.; Pan, D.; Cheang, P. Microstructure and mechanical  
47 properties of plasma sprayed HA/YSZ/Ti-6Al-4V composite coatings. *Biomaterials* 2004, 25,  
48 4009-4017.  
49  
50  
51  
52  
53  
54  
55  
56  
57  
58  
59  
60

- 1  
2  
3 7. van Oirschot, B. A.; Alghamdi, H. S.; Narhi, T. O.; Anil, S.; Al Farraj Aldosari, A.;  
4  
5 van den Beucken, J. J.; Jansen, J. A. In vivo evaluation of bioactive glass-based coatings on  
6  
7 dental implants in a dog implantation model. *Clin. Oral Implants Res.* 2014, 25, 21-28.
- 8  
9  
10 8. Cattini, A.; Latka, L.; Bellucci, D.; Bolelli, G.; Sola, A.; Lusvarghi, L.; Pawlowski,  
11  
12 L.; Cannillo, V. Suspension plasma sprayed bioactive glass coatings: Effects of processing on  
13  
14 microstructure, mechanical properties and in-vitro behaviour. *Surf. Coat Tech.* 2013, 220, 52-  
15  
16 59.
- 17  
18  
19 9. Monsalve, M.; Ageorges, H.; Lopez, E.; Vargas, F.; Bolivar, F. Bioactivity and  
20  
21 mechanical properties of plasma-sprayed coatings of bioglass powders. *Surf. Coat Tech.*  
22  
23 2013, 220, 60-66.
- 24  
25  
26 10. Cannillo, V.; Pierli, F.; Sampath, S.; Siligardi, C. Thermal and physical  
27  
28 characterisation of apatite/wollastonite bioactive glass-ceramics. *J. Europ. Ceram. Soc.* 2009,  
29  
30 29, 611-619.
- 31  
32  
33 11. Al-Noaman, A.; Rawlinson, S. C. F.; Hill, R. G. Bioactive glass-stoichiometric  
34  
35 wollastonite glass alloys to reduce TEC of bioactive glass coatings for dental implants.  
36  
37 *Mater. Lett.* 2013, 94, 69-71.
- 38  
39  
40 12. Deshpande, S.; James, A. W.; Blough, J.; Donneys, A.; Wang, S. C.; Cederna, P. S.;  
41  
42 Buchman, S. R.; Levi, B. Reconciling the effects of inflammatory cytokines on mesenchymal  
43  
44 cell osteogenic differentiation. *J. Surg. Res.* 2013, 185, 278-285.
- 45  
46  
47 13. Wu, X.; Wang, W.; Meng, C.; Yang, S.; Duan, D.; Xu, W.; Liu, X.; Tang, M.; Wang,  
48  
49 H. Regulation of differentiation in trabecular bonederived mesenchymal stem cells by T cell  
50  
51 activation and inflammation. *Oncol. Rep.* 2013, 30, 2211-2219.
- 52  
53  
54 14. Wu, G.; Liu, Y.; Iizuka, T.; Hunziker, E. B. The effect of a slow mode of BMP-2  
55  
56 delivery on the inflammatory response provoked by bone-defect-filling polymeric scaffolds.  
57  
58 *Biomaterials* 2010, 31, 7485-7493.
- 59  
60

- 1  
2  
3 15. Fellah, B. H.; Josselin, N.; Chappard, D.; Weiss, P.; Layrolle, P. Inflammatory  
4 reaction in rats muscle after implantation of biphasic calcium phosphate micro particles. *J*  
5 *Mater. Sci. Mater. Med.* 2007, 18, 287-294.  
6  
7  
8  
9  
10 16. Moon, H. J.; Yun, Y. P.; Han, C. W.; Kim, M. S.; Kim, S. E.; Bae, M. S.; Kim, G. T.;  
11 Choi, Y. S.; Hwang, E. H.; Lee, J. W.; Lee, J. M.; Lee, C. H.; Kim, D. S.; Kwon, I. K. Effect  
12 of heparin and alendronate coating on titanium surfaces on inhibition of osteoclast and  
13 enhancement of osteoblast function. *Biochem. Biophys. Res. Commun.* 2011, 413, 194-200.  
14  
15  
16  
17 17. Mouline, C. C.; Quincey, D.; Laugier, J. P.; Carle, G. F.; Bouler, J. M.; Rochet, N.;  
18 Scimeca, J. C. Osteoclastic differentiation of mouse and human monocytes in a plasma  
19 clot/biphasic calcium phosphate microparticles composite. *Eur. Cell Mater.* 2010, 20, 379-  
20 392.  
21  
22  
23  
24  
25  
26  
27 18. Lu, Y. P.; Li, M. S.; Li, S. T.; Wang, Z. G.; Zhu, R. F. Plasma-sprayed  
28 hydroxyapatite+titanium composite bond coat for hydroxyapatite coating on titanium substrate.  
29 *Biomaterials* 2004, 25, 4393-4403.  
30  
31  
32  
33 19. Yi, D.; Wu, C.; Ma, X.; Ji, H.; Zheng, X.; Chang, J. Preparation and in vitro  
34 evaluation of plasma-sprayed bioactive akermanite coatings. *Biomed. Mater.* 2012, 7,  
35 065004.  
36  
37  
38  
39  
40 20. Li, K.; Yu, J.; Xie, Y.; Huang, L.; Ye, X.; Zheng, X. Chemical stability and  
41 antimicrobial activity of plasma sprayed bioactive  $\text{Ca}_2\text{ZnSi}_2\text{O}_7$  coating. *J. Mater. Sci. Mater.*  
42 *Med.* 2011, 22, 2781-2789.  
43  
44  
45  
46  
47 21. Walschus, U.; Hoene, A.; Neumann, H. G.; Wilhelm, L.; Lucke, S.; Luthen, F.;  
48 Rychly, J.; Schlosser, M. Morphometric immunohistochemical examination of the  
49 inflammatory tissue reaction after implantation of calcium phosphate-coated titanium plates  
50 in rats. *Acta Biomater.* 2009, 5, 776-784.  
51  
52  
53  
54  
55  
56  
57  
58  
59  
60

- 1  
2  
3 22. Jakobsen, S. S.; Larsen, A.; Stoltenberg, M.; Bruun, J. M.; Soballe, K. Hydroxyapatite  
4 coatings did not increase TGF-beta and BMP-2 secretion in murine J774A.1 macrophages,  
5 but induced a pro-inflammatory cytokine response. *J. Biomater. Sci. Polym. Ed* 2009, 20,  
6 455-465.  
7  
8  
9  
10  
11 23. Iverson, N. M.; Plourde, N. M.; Sparks, S. M.; Wang, J.; Patel, E. N.; Shah, P. S.;  
12 Lewis, D. R.; Zablocki, K. R.; Nackman, G. B.; Uhrich, K. E.; Moghe, P. V. Dual use of  
13 amphiphilic macromolecules as cholesterol efflux triggers and inhibitors of macrophage  
14 athero-inflammation. *Biomaterials* 2011, 32, 8319-8327.  
15  
16  
17  
18  
19  
20 24. Alexander, K. A.; Chang, M. K.; Maylin, E. R.; Kohler, T.; Muller, R.; Wu, A. C.;  
21 Van Rooijen, N.; Sweet, M. J.; Hume, D. A.; Raggatt, L. J.; Pettit, A. R. Osteal macrophages  
22 promote in vivo intramembranous bone healing in a mouse tibial injury model. *J. Bone*  
23 *Miner. Res.* 2011, 26, 1517-1532.  
24  
25  
26  
27  
28  
29 25. Chang, M. K.; Raggatt, L. J.; Alexander, K. A.; Kuliwaba, J. S.; Fazzalari, N. L.;  
30 Schroder, K.; Maylin, E. R.; Ripoll, V. M.; Hume, D. A.; Pettit, A. R. Osteal tissue  
31 macrophages are intercalated throughout human and mouse bone lining tissues and regulate  
32 osteoblast function in vitro and in vivo. *J. Immunol.* 2008, 181, 1232-1244.  
33  
34  
35  
36  
37  
38 26. Pettit, A. R.; Chang, M. K.; Hume, D. A.; Raggatt, L. J. Osteal macrophages: a new  
39 twist on coupling during bone dynamics. *Bone* 2008, 43, 976-982.  
40  
41  
42  
43 27. Honda, Y.; Anada, T.; Kamakura, S.; Nakamura, M.; Sugawara, S.; Suzuki, O.  
44 Elevated extracellular calcium stimulates secretion of bone morphogenetic protein 2 by a  
45 macrophage cell line. *Biochem. Biophys. Res.* 2006, 345, 1155-1160.  
46  
47  
48  
49 28. Wahl, S. M.; McCartney-Francis, N.; Allen, J. B.; Dougherty, E. B.; Dougherty, S. F.  
50 Macrophage production of TGF-beta and regulation by TGF-beta. *Ann. N.Y. Acad. Sci.*  
51 1990, 593, 188-196.  
52  
53  
54  
55  
56  
57  
58  
59  
60

- 1  
2  
3 29. Chen, Z.; Wu, C.; Gu, W.; Klein, T.; Crawford, R.; Xiao, Y. Osteogenic  
4 differentiation of bone marrow MSCs by  $\beta$ -tricalcium phosphate stimulating macrophages via  
5 BMP2 signalling pathway. *Biomaterials* 2014, 35, 1507-1518.  
6  
7  
8  
9  
10 30. Walsh, M. C.; Kim, N.; Kadono, Y.; Rho, J.; Lee, S. Y.; Lorenzo, J.; Choi, Y.  
11 Osteoimmunology: interplay between the immune system and bone metabolism. *Annu. Rev.*  
12 *Immunol.* 2006, 24, 33-63.  
13  
14  
15  
16 31. Buache, E.; Velard, F.; Bauden, E.; Guillaume, C.; Jallot, E.; Nedelec, J. M.; Laurent-  
17 Maquin, D.; Laquerriere, P. Effect of strontium-substituted biphasic calcium phosphate on  
18 inflammatory mediators production by human monocytes. *Acta Biomater.* 2012, 8, 3113-  
19 3119.  
20  
21  
22  
23  
24  
25 32. Sugimoto, J.; Romani, A. M.; Valentin-Torres, A. M.; Luciano, A. A.; Ramirez  
26 Kitchen, C. M.; Funderburg, N.; Mesiano, S.; Bernstein, H. B. Magnesium decreases  
27 inflammatory cytokine production: a novel innate immunomodulatory mechanism. *J.*  
28 *Immunol.* 2012, 188, 6338-6346.  
29  
30  
31  
32  
33  
34 33. Shorr, E.; Carter, A. C. The usefulness of strontium as an adjuvant to calcium in the  
35 remineralization of the skeleton in man. *Bull Hosp. Joint Dis.* 1952, 13, 59-66.  
36  
37  
38 34. Wu, C.; Zhou, Y.; Lin, C.; Chang, J.; Xiao, Y. Strontium-containing mesoporous  
39 bioactive glass scaffolds with improved osteogenic/cementogenic differentiation of  
40 periodontal ligament cells for periodontal tissue engineering. *Acta Biomater.* 2012, 8, 3805-  
41 3815.  
42  
43  
44  
45  
46  
47 35. Zhang, Y.; Wei, L.; Chang, J.; Miron, R.; Shi, B.; Yi, S.; Wu, C. Strontium-  
48 incorporated mesoporous bioactive glass scaffolds stimulating in vitro proliferation and  
49 differentiation of bone marrow stromal cells and in vivo regeneration of osteoporotic bone  
50 defects. *J. mate. Chem. B* 2013, 1, 5711-5722.  
51  
52  
53  
54  
55  
56  
57  
58  
59  
60

- 1  
2  
3 36. Romer, P.; Desaga, B.; Proff, P.; Faltermeier, A.; Reicheneder, C. Strontium promotes  
4 cell proliferation and suppresses IL-6 expression in human PDL cells. *Ann. Anat.* 2012, 194,  
5 208-211.  
6  
7  
8  
9 37. Wallach, S. Effects of Magnesium on Skeletal Metabolism. *Magnesium Trace Elem.*  
10 1990, 9, 1-14.  
11  
12 38. Sojka, J. E.; Weaver, C. M. Magnesium supplementation and osteoporosis. *Nutrition*  
13 *Reviews* 1995, 53, 71-74.  
14  
15  
16 39. Kuno, T.; Hatano, Y.; Tomita, H.; Hara, A.; Hirose, Y.; Hirata, A.; Mori, H.;  
17 Terasaki, M.; Masuda, S.; Tanaka, T. Organomagnesium suppresses inflammation-associated  
18 colon carcinogenesis in male Crj: CD-1 mice. *Carcinogenesis* 2013, 34, 361-369.  
19  
20  
21 40. Carlisle, E. M. Silicon: a possible factor in bone calcification. *Science* 1970, 167,  
22 279-280.  
23  
24  
25 41. Xynos, I. D.; Edgar, A. J.; Buttery, L. D.; Hench, L. L.; Polak, J. M. Ionic products of  
26 bioactive glass dissolution increase proliferation of human osteoblasts and induce insulin-like  
27 growth factor II mRNA expression and protein synthesis. *Biochem. Biophys. Res. Commun.*  
28 2000, 276, 461-465.  
29  
30 42. Xynos, I. D.; Edgar, A. J.; Buttery, L. D.; Hench, L. L.; Polak, J. M. Gene-expression  
31 profiling of human osteoblasts following treatment with the ionic products of Bioglass 45S5  
32 dissolution. *J. Biomed. Mater. Res.* 2001, 55, 151-157.  
33  
34  
35 43. Wu, C. T.; Han, P. P.; Xu, M. C.; Zhang, X. F.; Zhou, Y. H.; Xue, G. D.; Chang, J.;  
36 Xiao, Y. Nagelschmidite bioceramics with osteostimulation properties: material chemistry  
37 activating osteogenic genes and WNT signalling pathway of human bone marrow stromal  
38 cells. *J. Mater. Chem. B* 2013, 1, 876-885.  
39  
40  
41  
42  
43  
44  
45  
46  
47  
48  
49  
50  
51  
52  
53  
54  
55  
56  
57  
58  
59  
60

- 1  
2  
3 44. Zhang, M.; Wu, C.; Lin, K.; Fan, W.; Chen, L.; Xiao, Y.; Chang, J. Biological  
4 responses of human bone marrow mesenchymal stem cells to Sr-M-Si (M = Zn, Mg) silicate  
5 bioceramics. *J. Biomed. Mater. Res. A* 2012, 100, 2979-2990.  
6  
7  
8  
9  
10 45. Kokubo, T.; Takadama, H. How useful is SBF in predicting in vivo bone bioactivity?  
11 *Biomaterials* 2006, 27, 2907-2915.  
12  
13  
14 46. Collin-Osdoby, P.; Osdoby, P. RANKL-mediated osteoclast formation from murine  
15 RAW 264.7 cells. *Methods Mol. Biol.* 2012, 816, 187-202.  
16  
17  
18 47. Wu, C.; Zhou, Y.; Xu, M.; Han, P.; Chen, L.; Chang, J.; Xiao, Y. Copper-containing  
19 mesoporous bioactive glass scaffolds with multifunctional properties of angiogenesis  
20 capacity, osteostimulation and antibacterial activity. *Biomaterials* 2013, 34, 422-433.  
21  
22  
23 48. Mareddy, S.; Crawford, R.; Brooke, G.; Xiao, Y. Clonal isolation and characterization  
24 of bone marrow stromal cells from patients with osteoarthritis. *Tissue Eng.* 2007, 13, 819-  
25 829.  
26  
27  
28 49. Singh, M. K.; Shokuhfar, T.; Gracio, J. J. D.; de Sousa, A. C. M.; Ferreira, J. M. D.;  
29 Garmestani, H.; Ahzi, S. Hydroxyapatite modified with carbon-nanotube-reinforced  
30 poly(methyl methacrylate): A nanocomposite material for biomedical applications. *Adv.*  
31 *Func. Mater.* 2008, 18, 694-700.  
32  
33  
34 50. Xiao, Y.; Haase, H.; Young, W. G.; Bartold, P. M. Development and transplantation  
35 of a mineralized matrix formed by osteoblasts in vitro for bone regeneration. *Cell Transplant*  
36 2004, 13, 15-25.  
37  
38  
39 51. Bohner, M.; Galea, L.; Doebelin, N. Calcium phosphate bone graft substitutes:  
40 Failures and hopes. *J. Eur. Ceram. Soc.* 2012, 32, 2663-2671.  
41  
42  
43 52. Zheng, X.; Huang, M.; Ding, C., Bond strength of plasma-sprayed hydroxyapatite/Ti  
44 composite coatings. *Biomaterials* 2000, 21, 841-849.  
45  
46  
47  
48  
49  
50  
51  
52  
53  
54  
55  
56  
57  
58  
59  
60



- 1  
2  
3 53. De, A. Wnt/Ca<sup>2+</sup> signaling pathway: a brief overview. *Acta Bioch. Bioph. Sin.* 2011,  
4  
5 43, 745-756.  
6  
7 54. Franz, S.; Rammelt, S.; Scharnweber, D.; Simon, J. C. Immune responses to implants  
8  
9 - a review of the implications for the design of immunomodulatory biomaterials. *Biomaterials*  
10  
11 2011, 32, 6692-6709.  
12  
13 55. Pearl, J. I.; Ma, T.; Irani, A. R.; Huang, Z.; Robinson, W. H.; Smith, R. L.; Goodman,  
14  
15 S. B. Role of the Toll-like receptor pathway in the recognition of orthopedic implant wear-  
16  
17 debris particles. *Biomaterials* 2011, 32, 5535-5542.  
18  
19 56. Kawai, T.; Akira, S. The role of pattern-recognition receptors in innate immunity:  
20  
21 update on Toll-like receptors. *Nat. Immunol.* 2010, 11, 373-384.  
22  
23 57. Zhou, H.; Zhao, K.; Li, W.; Yang, N.; Liu, Y.; Chen, C.; Wei, T. The interactions  
24  
25 between pristine graphene and macrophages and the production of cytokines/chemokines via  
26  
27 TLR- and NF-kappaB-related signaling pathways. *Biomaterials* 2012, 33, 6933-6942.  
28  
29 58. Nakamura, M.; Nagai, A.; Hentunen, T.; Salonen, J.; Sekijima, Y.; Okura, T.;  
30  
31 Hashimoto, K.; Toda, Y.; Monma, H.; Yamashita, K. Surface electric fields increase  
32  
33 osteoblast adhesion through improved wettability on hydroxyapatite electret. *ACS Appl.*  
34  
35 *Mater. Interfaces* 2009, 1, 2181-2189.  
36  
37 59. Zaidi, M. Skeletal remodeling in health and disease. *Nat Med* 2007, 13, 791-801.  
38  
39 60. Wright, H. L.; McCarthy, H. S.; Middleton, J.; Marshall, M. J. RANK, RANKL and  
40  
41 osteoprotegerin in bone biology and disease. *Curr. Rev. Musculoskelet Med* 2009, 2, 56-64.  
42  
43 61. Boyce, B. F.; Xing, L. Biology of RANK, RANKL, and osteoprotegerin. *Arthritis*  
44  
45 *Res. Ther.* 2007, 9, S1.  
46  
47 62. Gentleman, E.; Fredholm, Y. C.; Jell, G.; Lotfibakhshaiesh, N.; O'Donnell, M. D.;  
48  
49 Hill, R. G.; Stevens, M. M. The effects of strontium-substituted bioactive glasses on  
50  
51 osteoblasts and osteoclasts in vitro. *Biomaterials* 2010, 31, 3949-3956.  
52  
53  
54  
55  
56  
57  
58  
59  
60

- 1  
2  
3 63. Peng, S.; Liu, X. S.; Huang, S.; Li, Z.; Pan, H.; Zhen, W.; Luk, K. D.; Guo, X. E.; Lu,  
4  
5 W. W. The cross-talk between osteoclasts and osteoblasts in response to strontium treatment:  
6  
7 involvement of osteoprotegerin. *Bone* 2011, 49, 1290-1298.  
8  
9  
10 64. Yoshitake, F.; Itoh, S.; Narita, H.; Ishihara, K.; Ebisu, S. Interleukin-6 directly  
11  
12 inhibits osteoclast differentiation by suppressing receptor activator of NF-kappaB signaling  
13  
14 pathways. *J. Biol. Chem.* 2008, 283, 11535-11540.  
15  
16  
17 65. Axmann, R.; Bohm, C.; Kronke, G.; Zwerina, J.; Smolen, J.; Schett, G. Inhibition of  
18  
19 interleukin-6 receptor directly blocks osteoclast formation in vitro and in vivo. *Arthritis*  
20  
21 *Rheum.* 2009, 60, 2747-2756.  
22  
23  
24 66. Palmqvist, P.; Persson, E.; Conaway, H. H.; Lerner, U. H. IL-6, leukemia inhibitory  
25  
26 factor, and oncostatin M stimulate bone resorption and regulate the expression of receptor  
27  
28 activator of NF-kappa B ligand, osteoprotegerin, and receptor activator of NF-kappa B in  
29  
30 mouse calvariae. *J. Immunol.* 2002, 169, 3353-3362.  
31  
32  
33 67. Richardson, I. G. The nature of the hydration products in hardened cement pastes.  
34  
35 *Cem. Concr. Comp.* 2000, 22, 97-113.  
36  
37  
38 68. Li, J.; Song, Y.; Zhang, S.; Zhao, C.; Zhang, F.; Zhang, X.; Cao, L.; Fan, Q.; Tang, T.  
39  
40 In vitro responses of human bone marrow stromal cells to a fluoridated hydroxyapatite coated  
41  
42 biodegradable Mg-Zn alloy. *Biomaterials* 2010, 31, 5782-5788.  
43  
44  
45 69. Costa, D. O.; Prowse, P. D.; Chrones, T.; Sims, S. M.; Hamilton, D. W.; Rizkalla, A.  
46  
47 S.; Dixon, S. J. The differential regulation of osteoblast and osteoclast activity by surface  
48  
49 topography of hydroxyapatite coatings. *Biomaterials* 2013, 34, 7215-7226.  
50  
51  
52  
53  
54  
55  
56  
57  
58  
59  
60

		Culture medium immersed				Macrophage conditioned				Osteoclast conditioned			
		HA		SrMg		HA		SrMg		HA		SrMg	
		0-3 d	3-6 d	0-3 d	3-6 d	0-3 d	3-6 d	0-3 d	3-6 d	0-3 d	3-6 d	0-3 d	3-6 d
Ionic concentrations (mg/ L)	Ca	20.19±0.31	17.75±0.53	0.46±0.01	16.69±1.25	29.89±0.21	25.11±0.49	0.32±0.01	18.07±0.02	26.81±0.46	24.93±0.23	0.20±0.02	17.01±0.36
	P	5.31±0.08	5.15±3.08	1.78±0.16	7.11±0.22	4.54±0.26	5.08±0.12	1.51±0.11	7.72±0.09	4.54±0.18	5.08±0.12	1.40±0.09	6.85±0.16
	Si	0.42±0.02	0.22±0.02	24.51±0.85	19.03±0.21	0.43±0.04	0.18±0.01	29.46±0.11	20.02±0.35	0.41±0.02	0.15±0.02	24.88±0.17	19.20±0.49
	Sr	0.26±0.05	0.33±0.11	2.97±0.02	102.06±0.13	0.17±0.14	0.25±0.03	7.49±0.13	134.23±1.38	0.16±0.02	0.21±0.10	5.88±0.19	151.02±3.26
	Mg	1.51±0.03	2.70±0.09	75.97±1.95	21.66±0.34	2.38±0.08	3.53±0.08	73.25±2.16	22.06±0.28	1.90±0.08	3.28±0.05	74.12±0.08	22.66±0.41

Table 1. The ionic concentrations of medium for SMS and HA coatings at different culture conditions.

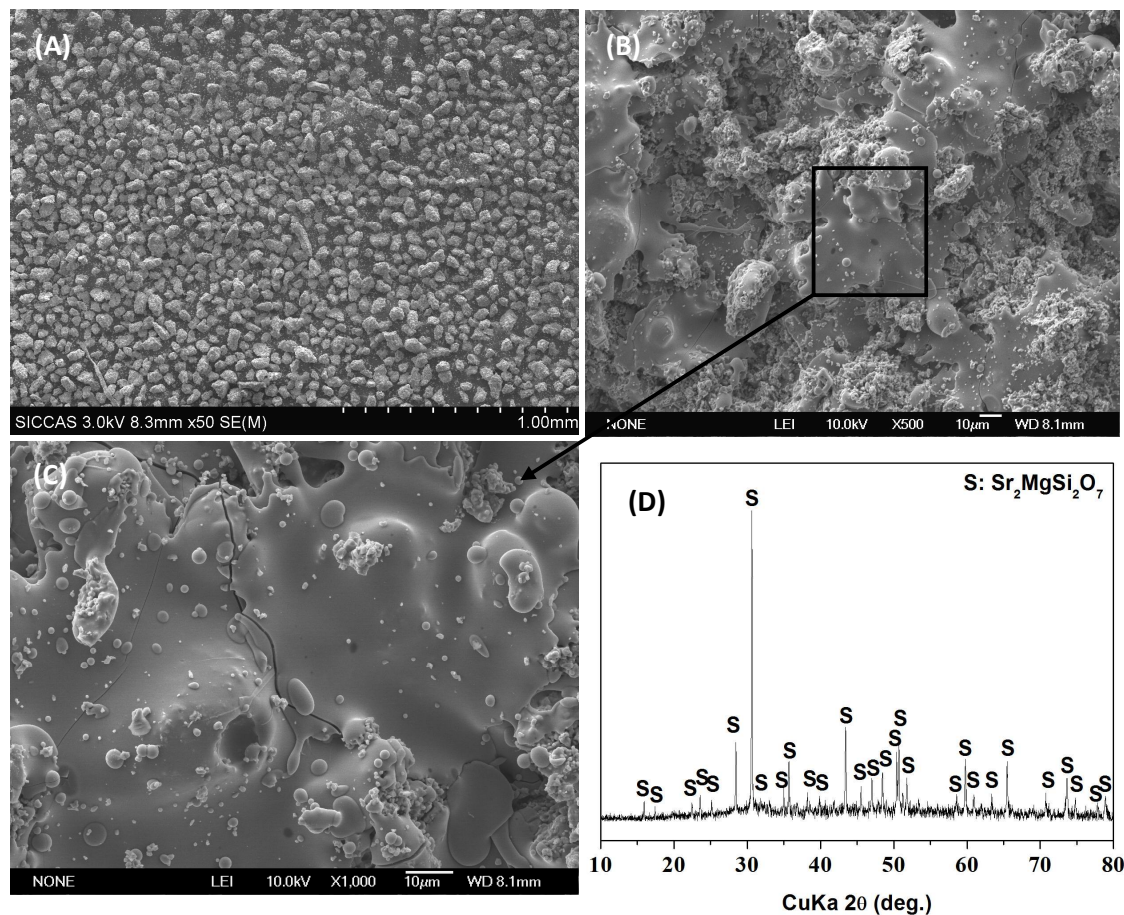


Figure 1. SEM for the prepared  $\text{Sr}_2\text{MgSi}_2\text{O}_7$  particles (A) and coatings (B, C). (C) is higher magnification image of (B). XRD analysis for the prepared  $\text{Sr}_2\text{MgSi}_2\text{O}_7$  coatings on Ti alloys (D), in which S stands for the characteristic peaks of crystal phase  $\text{Sr}_2\text{MgSi}_2\text{O}_7$  in the XRD pattern.

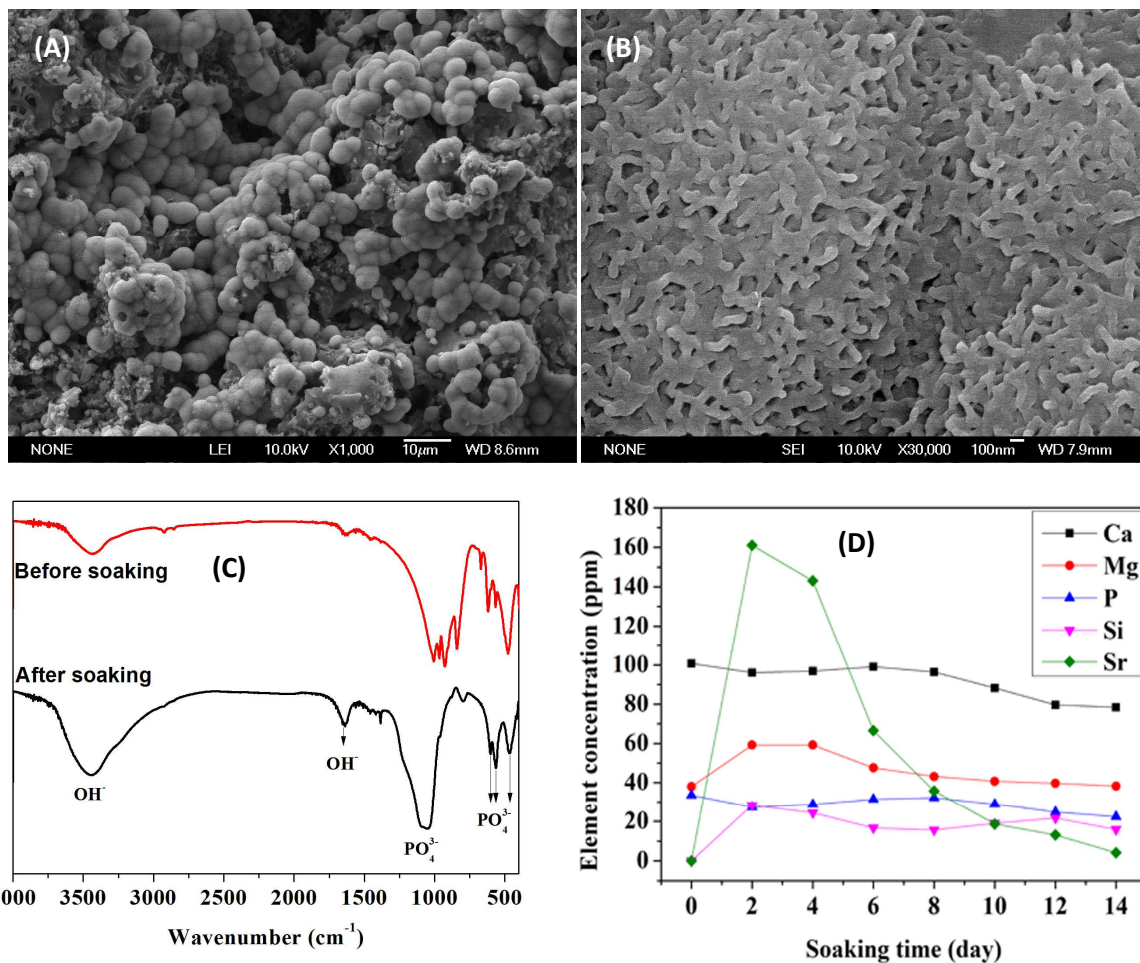


Figure 2. SEM (A, B) and FTIR (C) analysis for the prepared  $\text{Sr}_2\text{MgSi}_2\text{O}_7$  coatings on Ti alloys after soaked in SBF for 14 days. ICP-AES analysis for the change of ionic concentrations in SBF soaked with  $\text{Sr}_2\text{MgSi}_2\text{O}_7$  coatings (D).

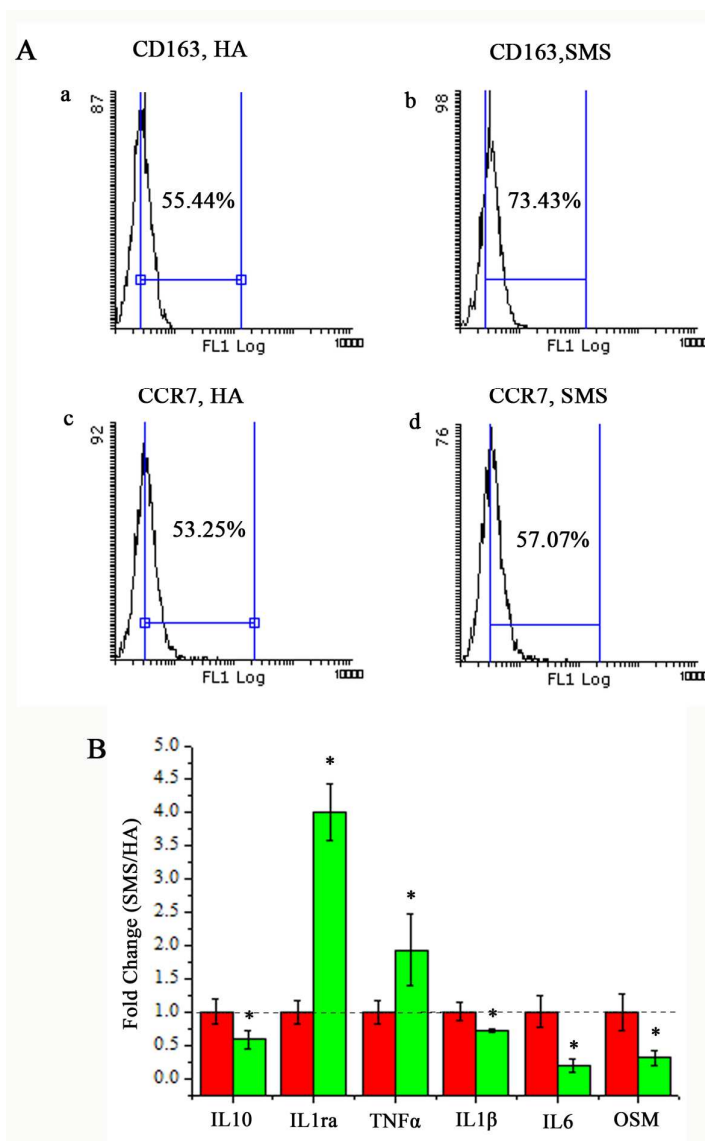


Figure 3. (A). FACS results of RAW 264.7 cells cultured in different coatings. The mean fluorescence intensity of CD163 increased after the stimulation of SMS (a, b); however, the mean fluorescence intensity of CCR7 had only slight increase under the same treatment (c, d). (B). Fold changes of inflammation related genes IL10, IL1ra, TNF $\alpha$ , IL1 $\beta$ , IL6 and OSM, by comparing RAW 264.7 cells cultured in SMS coating with HA (HA group has been standardized as 1, see red bar). \*: Significant difference (P < 0.05).

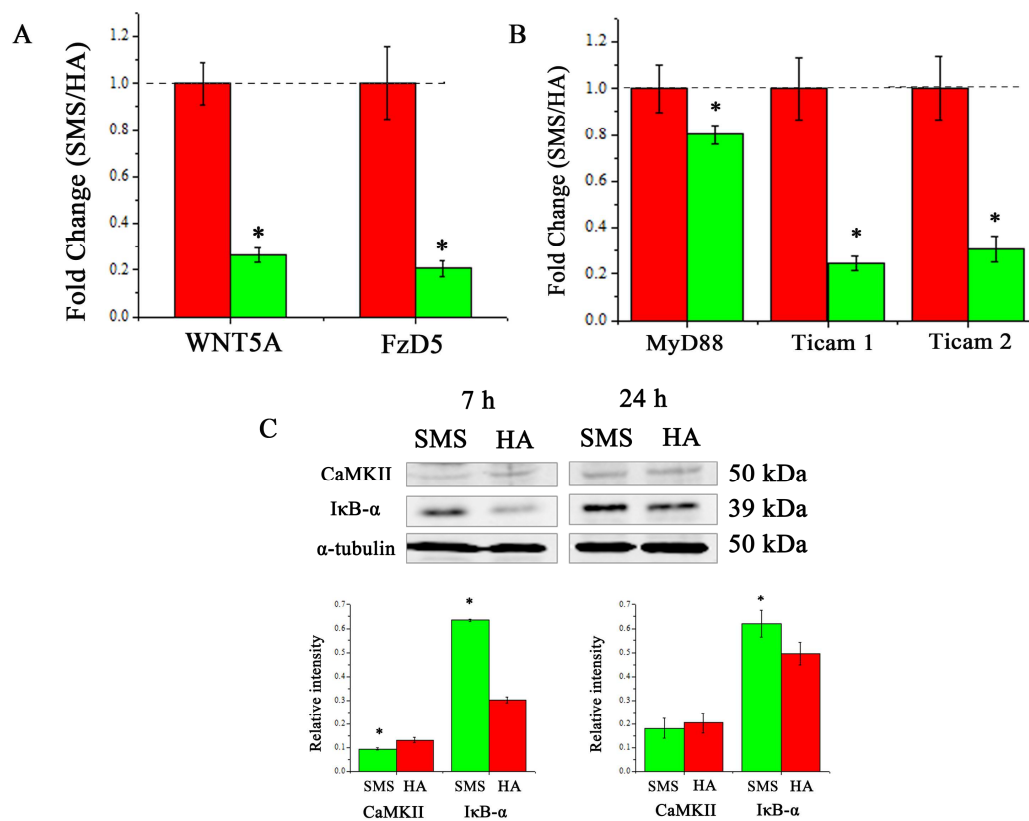


Figure 4. (A) Fold changes of WNT5A/Ca<sup>2+</sup> pathway related genes: WNT5A and Fz5; (B) Fold changes of Toll-like pathway related genes: MyD88, Ticam1 and Ticam2; (C). Western blotting analysis of CaMKII and IκB-α expression. \*: Significant difference by comparing RAW 264.7 cells cultured in SMS coating with HA (P < 0.05). (HA group has been standardized as 1, see red bar in Figure A and B).

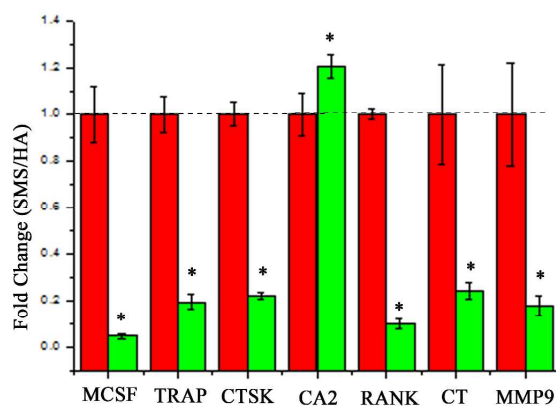


Figure 5. Fold changes of osteoclastogenesis and osteoclast activities related genes: MCSF, TRAP, CTSK, CA2, RANK, CT and MMP9. \*: Significant difference by comparing RAW 264.7 cells cultured in SMS coating with HA ( $P < 0.05$ ). (HA group has been standardized as 1, see red bar).



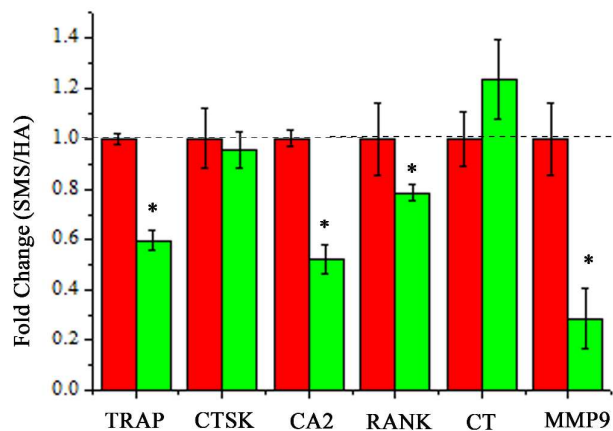


Figure 6. Fold changes of osteoclast activities related genes: TRAP, CTSK, CA2, RANK, CT and MMP9. \*: Significant difference by comparing RAW 264.7 cells derived osteoclasts cultured in SMS coating with HA ( $P < 0.05$ ). (HA group has been standardized as 1, see red bar).

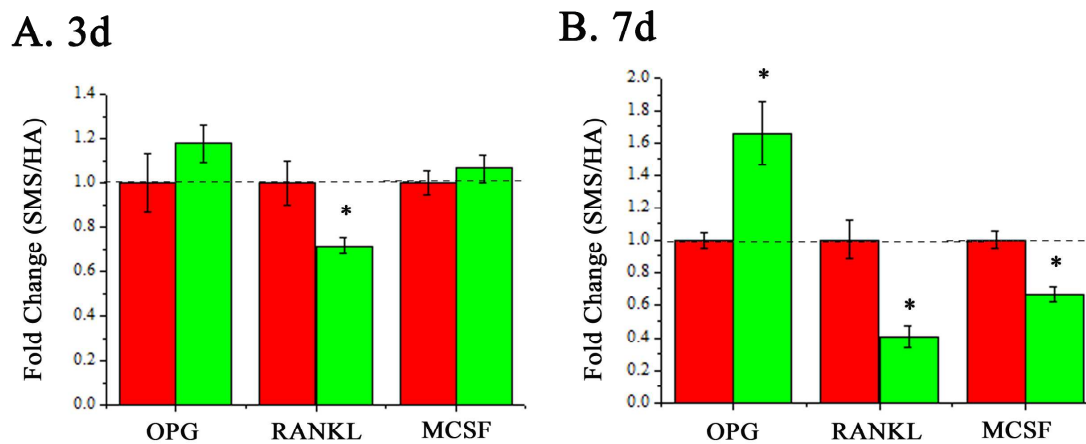


Figure 7. Fold changes of osteoclastogenesis related genes: OPG, RANKL, and MCSF. (A). Day 3, (B). Day 7. \*: Significant difference by comparing BMSCs cultured in SMS coating stimulated RAW 264.7 cells conditioned medium with HA coating stimulated RAW 264.7 cells conditioned medium ( $P < 0.05$ ). (HA group has been standardized as 1, see red bar).

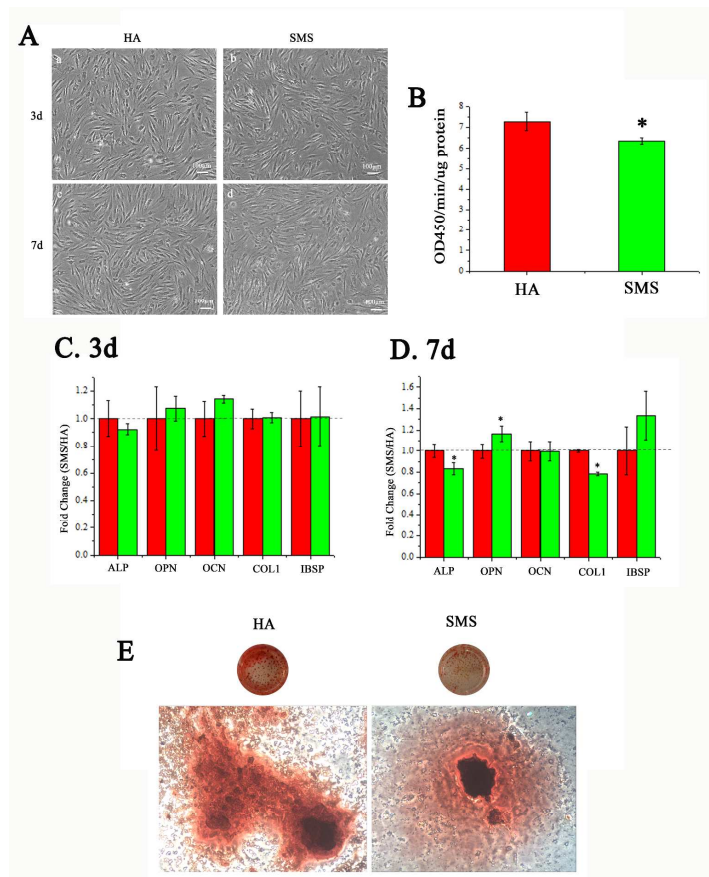


Figure 8. Osteogenic differentiation of BMSCs cultured in SMS and HA coatings stimulated RAW 264.7 cells conditioned medium. (A). morphologies of BMSCs in day 3 and 7; (B). ALP activities; (C&D). osteogenesis related gene expression (ALP, OPN, OCN, COL1, IBSP) by BMSCs in day 3 and 7; (E). alizarin red results. \*: Significant difference by comparing BMSCs cultured in SMS coatings stimulated RAW 264.7 cells conditioned medium with HA coatings stimulated RAW 264.7 cells conditioned medium ( $P < 0.05$ ). (HA group has been standardized as 1, see red bar).

## Table of contents graphic

Sr, Mg and Si-containing bioceramic coatings possess high bonding strength and osteogenic bioactivity for inhibiting inflammation, osteoclastogenesis

